Journal of Civil Engineering and Architecture 16 (2022) 137-149
doi: 10.17265/1934-7359/2022.03.003

# Proposal of Stainless Steel Roof Structure and Tiles for Gymnasiums

Géferson Diogo de Oliveira, Henor Artur de Souza, Rovadávia Aline de Jesus Ribas and Lucas Fonseca Caetano
*Federal University of Ouro Preto (UFOP)-University Campus, s/n, Morro do Cruzeiro, Ouro Preto, MG 35400-000, Brazil*

**Abstract:** This work proposed an architectural alternative project of a stainless steel roof structure that uses roof tiles also in stainless steel with emphasis on roofs for multi-sport gymnasiums. In the development of the work, two existing multi-sports gymnasiums are taken as a reference, but with ASTM (American Society for Testing and Materials) A36 steel roof structure. The proposed cover system uses cables and light gauge profiles, in commercial stainless steel, which reduces the weight and of course the final price of the roof structure. A structure that presents technical feasibility is obtained and analyzed by checking its behavior with respect to the efforts and displacements generated by the combinations of the acting loads, following the safety recommendations of the applicable standard. It is verified that using the stainless steel structure proposed in this work would cost 42% of the reference structure if this were in AISI (American Iron and Steel Institute) 304 stainless steel. And this cost tends to be minimized due to greater durability and consequent reduction in maintenance costs of this type of steel.

**Key words:** Stainless steel, roof structure, design, gymnasiums.

## 1. Introduction

The longevity and aesthetic appeal of stainless steel have inspired architects and designers to use the material in practical and imaginative ways. Stainless steel structural elements are increasingly being used in civil construction, especially in new constructions. In structural applications, the main types of alloys indicated are ferritic, austenitic, and also the latest duplex stainless steel [1-3].

Mechanical properties, such as hardening in the plastic phase and high ductility, make austenitic and duplex steels suitable for structures subjected to accidental loading. Stainless steel products are manufactured from plates, strips, tubes, bars, which result in cold and hot-rolled structural profiles, castings, clamping elements, and fasteners. For structural members, cold-formed profiles are normally used, mainly because they are more available than rolled ones, require relatively low investments to achieve production capacities, and are suitable for light structural applications with high structural efficiency [4].

In addition to structural performance, several other issues influence the choice of material for construction, and while stainless steel has a high initial material cost, it has additional beneficial properties that can provide cost savings in other respects. The factors that favor stainless steel as a material choice for use in structures are final cost, aesthetics, durability, behavior at high temperatures, reuse, long service life, contribution to the preservation of natural resources, cost of the entire service life, and recovery capacity.

In this context, this work proposes a design of a stainless steel roof structure from the study of two existing multi-sport gymnasiums, proposing a structure that has the same material as the tiles, that is, stainless steel, to obtain a building that presents greater resistance to the weather and, consequently, greater durability. This study aims to obtain a design alternative for the stainless steel roof structure that is light enough to reduce the amount of material, lowering, of course, its price, and at the same time is modern.

**Corresponding author:** Lucas Fonseca Caetano, PhD, professor, research fields: Civil engineering, Structural engineering, Building performance, Thermal performance.

## 2. Objective

The objective of this work is to propose a viable architectural design alternative of a lightweight stainless steel roof structure that also uses stainless steel tiles.

## 3. Materials and Methods

The adopted method for the development of this work encompasses the proposition of a stainless steel roof structure with the use of tiles also made of this material. From the proposed architectural project, an analysis of its structural behavior is made. Two existing multi-sport gymnasiums are taken as a reference, which have a roof structure in ASTM (American Society for Testing and Materials) A36 steel. To check the structural behavior of the proposed roof, three load combinations are considered: live load as the main variable, overpressure wind as the main variable, and suction wind as the main variable. The calculations are performed with the help of Visual Ventos™ and SAP2000™ programs. A cost analysis of the proposed model is also carried out.

### *3.1 Roofing Model Proposal*

The structure that makes up the roofs of the courts of the two multi-sport gymnasiums taken as a reference has several similarities from its architectural and structural design, its use, and also the problems of maintenance and natural wear and tear. Both are covered with AISI 304 stainless steel tiles, supported by an arched truss structure in ASTM A36 structural steel (Fig. 1a), with a yield stress of approximately 250 MPa and each arch weighing approximately 2,502 kg [5]. A structure model is suggested that is lighter and that preserves functional characteristics of multi-sport courts, such as wide spans and ceiling height suitable for the practice of sports (Fig. 1b).

The definition of the proposed roof structure project arises from the arrangement of the supports at the lateral ends, which allows for large free spans, creating a sequence of aligned porticos. An arrangement of smooth rectangular bars is chosen, highlighting the natural aesthetic characteristic of stainless steel. Cables, also in stainless steel, complement the structure with their functional and aesthetic character.

### *3.2 Definition of the Geometric Model*

Using buildings housing multi-sports courts as references and reviewing the architectural project of the two gymnasiums mentioned, it was chosen to design a space that will house two multi-sports courts, one main, with Olympic dimensions (40 m × 20 m), and another secondary, with dimensions also Olympic (18 m × 9 m), also considering the mandatory circulation and escape areas. Elements such as bleachers, changing rooms, bathrooms, among others, are disregarded, as it is a roofing project that takes into account the minimum dimensions to house such court.

(a) Gymnasium took as a reference.

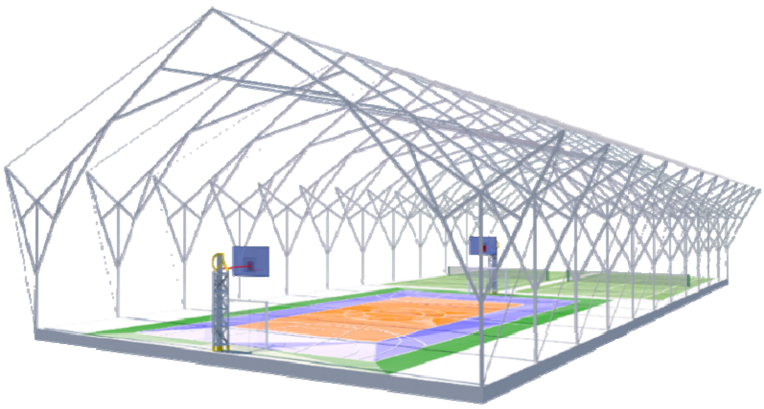

(b) Proposed structure model.

**Fig. 1 Structure of the multi-sport gymnasiums.**

Source: Oliveira [6].

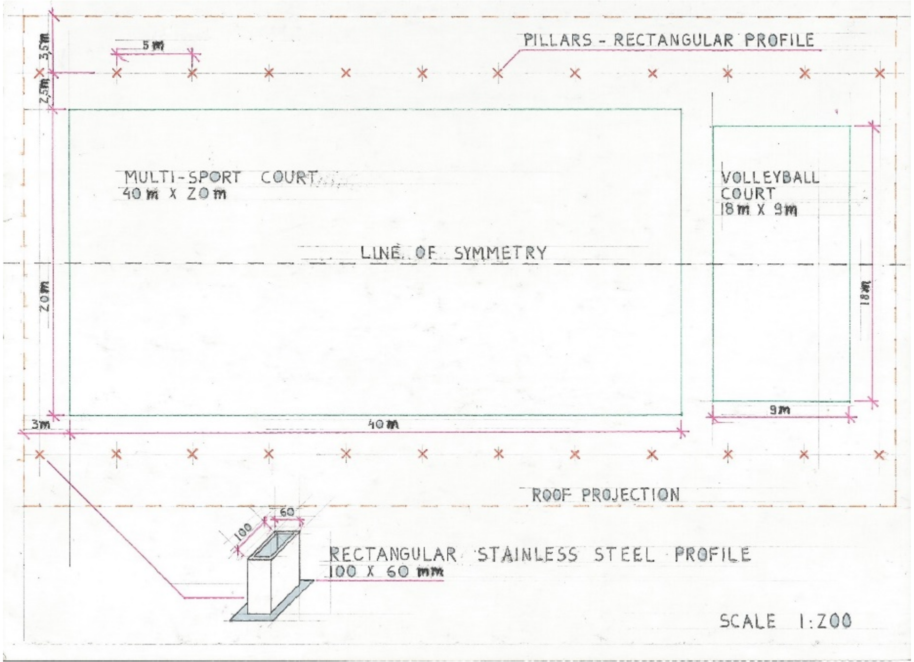


**Fig. 2 Drawing with technical information for project development.**
Source: Oliveira [6].

The measures that the roof must have are defined based on the dimensions of the internal courts of the existing gymnasiums, and linear dimensions of 55 m in length by 25 m in width are adopted. Fig. 2 shows a sketch prepared for the proposed project.

The stainless steel columns, of rectangular sections, are identical. All are lined up and evenly spaced from each other. The set of columns is replicated at the opposite side end, forming a symmetrical structure, having its mirror axis at the center of the building. As a result, twelve 5.83 m high columns are installed at each side, spaced 5 m apart, from center to center, forming eleven spans (Fig. 2).

The roofing structure of the building is also formed by rectangular stainless steel profiles and is responsible for supporting and giving the correct inclination to the stainless steel tiles. To define the nodes of the structure, a grid system is created, in which, by coordinates, it is possible to make this marking with greater precision. The coordinates are given in such a way that on the $x$-axis the linear dimensions are presented in the horizontal direction, expressed by Arabic numerals, and on the $y$-axis the linear dimensions are presented in the vertical direction, expressed by capital letters. The location of the structure node is called by the sequence $x$-$y$ corresponding to the coordinate (Fig. 3).

The roof shape is defined as main gable roof with the upper horizontal edges meeting to form the ridge and two other lateral sections in opposite directions, all with a 55% slope, as can be seen in Fig. 3. Two stainless steel gutters are provided for capturing and draining rainwater, located in the longitudinal direction of the roof.

### 3.3 Structural Design of the Roof

The porticos that make up the roof structure are formed by structural stainless steel profiles of rectangular section and 6 × 25 stainless steel cables, aligned and spaced every 5 m. These structures are fixed by means of steel anchors anchored in concrete blocks, while the profiles are welded together. The cables are fixed at the ends of the profiles. The stainless steel structural profiles must be properly welded together forming a mosaic composed of triangular figures (Fig. 3). These profiles have commercial dimensions of

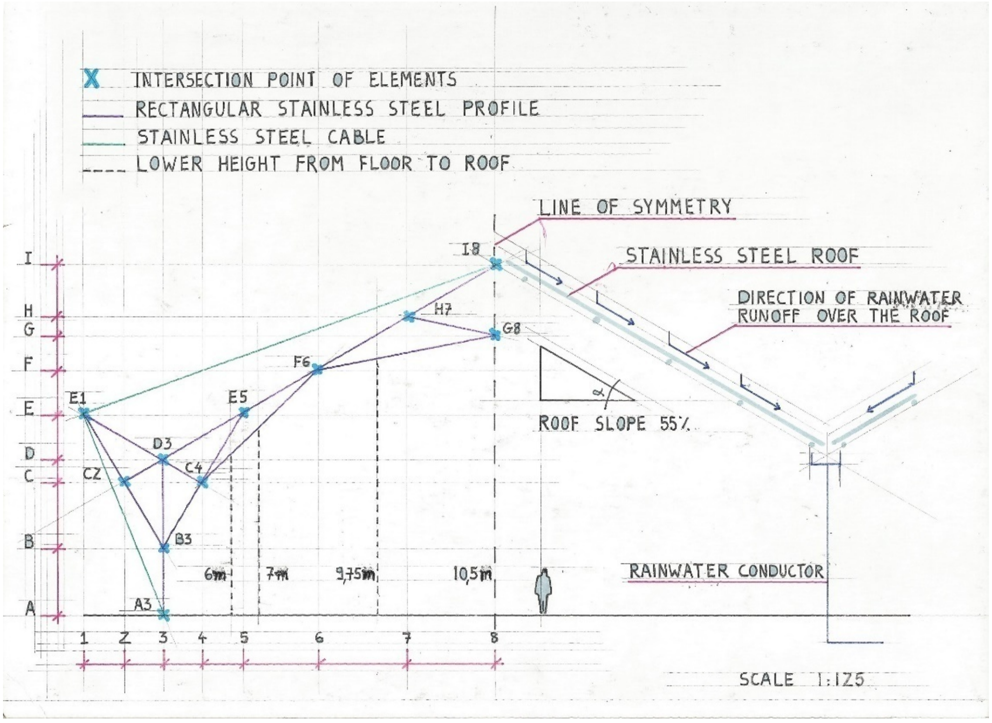


**Fig. 3 Drawing with relevant technical information for the development of the project.**
Source: Oliveira [6].

**Table 1 Properties of AISI 304 stainless steel.**

| Properties | Nominal value |
|---|---|
| Specific mass ($\gamma_{aço}$) | 79 kN/m³ |
| Young's modulus ($E$) | 200 GPa |
| Shear modulus ($G$) | 79 GPa |
| Poisson's ratio ($\nu$) | 0.28 |
| Yield strength ($f_y$) | 400 MPa |
| Tensile strength ($\sigma_r$) | 600 MPa |
| Coefficient of thermal expansion ($\alpha$) | $1.1 \times 10^{-5}$/K |
| Thermal conductivity ($\lambda$) | 14 W/(m·K) |
| Specific heat ($c$) | 440 J/(kg·K) |

Source: solidworks [7].

60 mm × 100 mm × 3 mm and 60 mm × 80 mm × 3 mm, while the 6 × 25 cables are 38 mm in diameter.

The stainless steel used in the project is AISI 304 austenitic steel, whose properties are shown in Table 1.

The rectangular profiles adopted are hot-rolled (Fig. 4a). The cables have a breaking load equal to 843.44 kN according to the NBR (Norma Brasileira) ISO (International Organization for Standardization) 2408 standard [8]. To verify the structure, an elastic-linear analysis is carried out and the supports of the columns and the connections between the bars of the structure are considered to be of the third type (rigid). The cable connections to the structure are considered to be of the second type (labeled) for better flexibility and deformation capacity of these structures [9].

The elements that make up the portico are named by capital letters in alphabetical order from bottom to top and from left to right. As it is a symmetrical structure, the nomenclature of the bars occurs only on one side, being of course equal to the opposite side. Bar elements A and E are treated as columns, elements C, D, F, G, H, I, J, K, L, N, O, P, Q, and R as beams, and elements B and M are cables. The total weight of one portico is 10.57 kN (Table 2; Fig. 4b).

### *3.4 Structural Analysis of the Proposed Roofing*

From the proposed architectural project, an analysis of its structural behavior is made. For this, a finite element mesh is defined, from which the slenderness of the elements is verified and the values of the requesting efforts are obtained, with the help of the

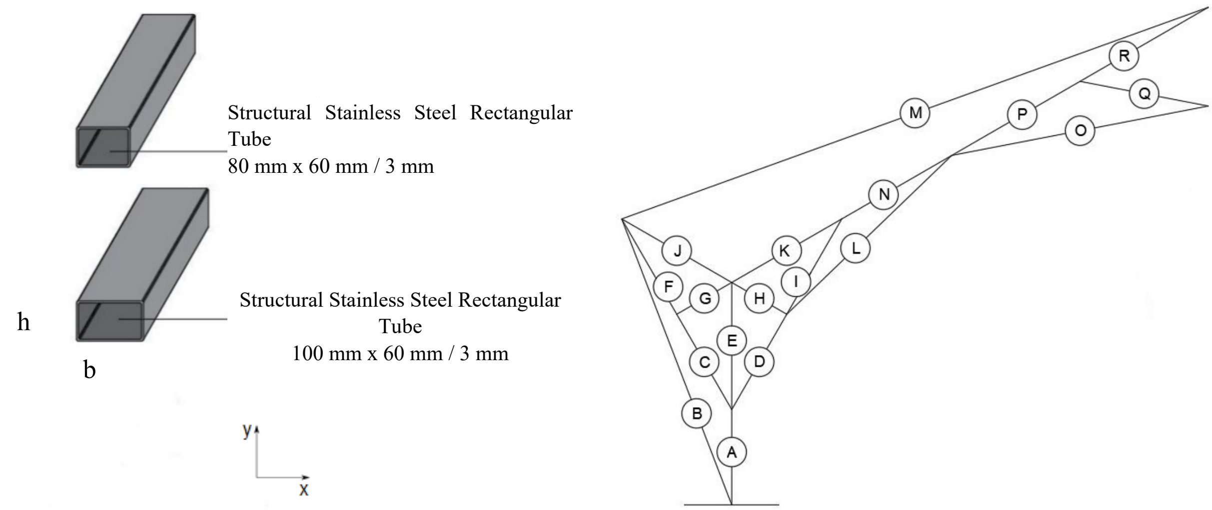


(a) Sections of the elements that make up the structure (b) Arrangement and naming of elements

**Fig. 4 Elements that make up the proposed frame and their sections.**

Source: Oliveira [6].

**Table 2 Details of the elements that make up the proposed frame.**

| Element | Section-Dimension (mm) | | | | Length (m) | Linear weight (kg/m) | Total weight (kg) |
|---|---|---|---|---|---|---|---|
| | Rectangular | | | Circular | | | |
| | *b* (base) | *h* (height) | *t* (thickness) | *Ø* (diameter) | | | |
| A | 100 | 60 | 3 | | 2.50 | 7.30 | 18.25 |
| B | - | - | - | 38 | 8.04 | 5.63 | 45.27 |
| C | 100 | 60 | 3 | - | 2.89 | 7.30 | 21.10 |
| D | 100 | 60 | 3 | - | 2.89 | 7.30 | 21.10 |
| E | 100 | 60 | 3 | - | 3.33 | 7.30 | 24.31 |
| F | 100 | 60 | 3 | - | 2.89 | 7.30 | 21.10 |
| G | 100 | 60 | 3 | - | 1.67 | 7.30 | 12.19 |
| H | 100 | 60 | 3 | - | 1.67 | 7.30 | 12.19 |
| I | 100 | 60 | 3 | - | 2.89 | 7.30 | 21.10 |
| J | 100 | 60 | 3 | - | 3.33 | 7.30 | 24.31 |
| K | 100 | 60 | 3 | - | 3.33 | 7.30 | 24.31 |
| L | 100 | 60 | 3 | - | 6.01 | 7.30 | 43.87 |
| M | - | - | - | 38 | 16.36 | 5.63 | 92.10 |
| N | 100 | 60 | 3 | - | 3.33 | 7.30 | 24.31 |
| O | 80 | 60 | 3 | - | 6.85 | 6.45 | 44.18 |
| P | 100 | 60 | 3 | - | 3.88 | 7.30 | 28.32 |
| Q | 80 | 60 | 3 | - | 3.20 | 6.45 | 22.05 |
| R | 100 | 60 | 3 | - | 3.88 | 7.30 | 28.32 |

Source: Oliveira [6].

SAP2000™ software, version 14.0.0. Table 3 presents the geometric properties of the rectangular sections used in SAP2000™ and in when checking the resistance of the elements, where *b* is the base, *h* is the height and *t* is the wall thickness of the profile, *A* is the cross-sectional area; *I* is the moment of inertia; *W* is the Young's modulus; *r* is the radius of gyration; *Z* is the plastic modulus; and *Q* is the static moment.

**Table 3 Geometric properties of rectangular sections.**

| Profile | Linear weight | $b$ | $h$ | $t$ | $A$ | $x$-$x$ axis | | | | | $y$-$y$ axis | | | |
|---|---|---|---|---|---|---|---|---|---|---|---|---|---|---|
| | | | | | | $I_x$ | $W_x$ | $r_x$ | $Z_x$ | $Q_x$ | $I_y$ | $W_y$ | $r_y$ | $Z_y$ |
| | kg/m | mm | mm | mm | mm$^2$ | mm$^4$ | cm$^3$ | mm | cm$^3$ | mm$^3$ | mm$^4$ | cm$^3$ | mm | cm$^3$ |
| 80 × 60 | 6.45 | 80 | 60 | 3 | 804 | 468972 | 15.63 | 24.15 | 18.05 | 36108 | 736492 | 18.41 | 30.27 | 22.07 |
| 100 × 60 | 7.3 | 100 | 60 | 3 | 924 | 566532 | 18.88 | 24.76 | 21.47 | 42945 | 1262372 | 25.25 | 36.96 | 30.71 |

Source: Oliveira [6].

For the structural analysis, a linear mesh of finite elements of dimension equal to 250 mm is defined, in the bar elements, from which, as the refinement is increased, there is no change in the results. Other profiles are also tested with their respective parameters. However, the profiles adopted are those that present satisfactory results to proceed with the design.

To verify that the profiles safely meet the demands imposed by the loads on the building, the recommendations stipulated by Eurocode 3 [10-14] are applied, since there are no specific Brazilian national standards for the design of stainless steel structures. The analysis considers, in addition to the more critical situation of requesting efforts, the recommendation on the maximum allowable displacements as a criterion for acceptance of the adopted profiles.

The requesting efforts are obtained from the significant actions that act on the structure, considering the dead load, constituted by the roof's weight, composed of the structure and other elements, such as tiles and purlins, and the variable load, constituted by the live load and wind load (Table 4).

The cables are subjected to the following axial forces, defining initial stresses in these elements: cable B on the left and right side and cable M on the left side: 1 kN; cable M on the right side: 1.5 kN. It is observed that in the right cable M, a higher value of initial tension is placed to maintain the symmetry of the structure's behavior and so that the same values of efforts are obtained on each side.

For the design in the ULS (Ultimate Limit State), three combinations of actions are performed and, to verify the maximum displacements foreseen in the structure, the SLS (Serviceability Limit State) is considered, in which the applied load is also defined by combinations of actions, according to the NBR 8800 standard [15]. The combinations of actions for the ULS and SLS are shown in Table 5. The load is evenly distributed over the structure.

**Table 4 Dead loads, live load and wind loads.**

| Type of load | Value |
|---|---|
| Dead load (self-weight) | 10.57 kN |
| Dead load (tiles and purlins) | 0.10 kN/m |
| Live load | 1.25 kN/m |
| Overpressure wind | 2.05 kN/m |
| Suction wind | 1.64 kN/m |

Source: Oliveira [6].

**Table 5 Load combinations considered in the structure analysis.**

| Limit state | Combination | Loading status |
|---|---|---|
| | CI (combination I) | Live load as main variable |
| ULS | CII (combination II) | Overpressure wind as main variable |
| | CIII (combination III) | Suction wind as main variable |
| | APC (almost permanent combination) | Dead load + 0.3 × Live load |
| SLS | FC1 (frequent combination 1) | Dead load + 0.4 × Live load |
| | FC2 (frequent combination 2) | Dead load + 0.3 × Wind Overpressure + 0.3 × Live load |

Source: Oliveira [6].

**Table 6 Elements slenderness index values.**

| Element | $L$ (m) | $L_f$ (m) | $r_x$ (m) | $\lambda_x$ | $r_y$ (m) | $\lambda_y$ |
|---|---|---|---|---|---|---|
| A | 2.5 | 1.250 | 0.02476 | 50.48 | 0.03696 | 33.82 |
| B | - | - | - | - | - | - |
| C | 2.89 | 1.445 | 0.02476 | 58.36 | 0.03696 | 39.10 |
| D | 2.89 | 1.445 | 0.02476 | 58.36 | 0.03696 | 39.10 |
| E | 3.33 | 1.665 | 0.02476 | 67.25 | 0.03696 | 45.05 |
| F | 2.89 | 1.445 | 0.02476 | 58.36 | 0.03696 | 39.10 |
| G | 1.67 | 0.835 | 0.02476 | 33.72 | 0.03696 | 22.59 |
| H | 1.67 | 0.835 | 0.02476 | 33.72 | 0.03696 | 22.59 |
| I | 2.89 | 1.445 | 0.02476 | 58.36 | 0.03696 | 39.10 |
| J | 3.33 | 1.665 | 0.02476 | 67.25 | 0.03696 | 45.05 |
| K | 3.33 | 1.665 | 0.02476 | 67.25 | 0.03696 | 45.05 |
| L | 6.01 | 3.005 | 0.02476 | 121.37 | 0.03696 | 81.30 |
| M | - | - | - | - | - | - |
| N | 3.33 | 1.665 | 0.02476 | 67.25 | 0.03696 | 45.05 |
| O | 6.85 | 3.425 | 0.02415 | 141.82 | 0.03027 | 113.15 |
| P | 3.88 | 1.940 | 0.02476 | 78.35 | 0.03696 | 52.49 |
| Q | 3.2 | 1.600 | 0.02415 | 66.25 | 0.03027 | 52.86 |
| R | 3.88 | 1.940 | 0.02476 | 78.35 | 0.03696 | 52.49 |

Source: Oliveira [6].

Table 6 shows the slenderness indices ($\lambda$) of the elements in relation to the $x$ and $y$ axes, where $L$ is the span of the part; $L_f$ is the buckling length, given by half the height of the elements because they are fixed; and $r$ is the radius of gyration.

Observing the results shown in Table 6, the slenderness index ($\lambda$) of all profiles is in accordance with Eurocode 3 [10-14], which defines as maximum limit values of the slenderness index equal to 250 for secondary or bracing elements, and equal to 180 for compressed elements in general.

## 4. Results and Discussion

This section presented the results obtained for the requesting efforts, which are the shear and normal forces, bending moments, and normal stresses, as well as the displacements, expected for each element that makes up the proposed structure, and each combination of external forces. Afterwards, the maximum values of these parameters are applied to check the resistance of the structure.

### *4.1 Requesting Efforts (Shear and Normal Forces)*

The maximum values of shear and normal forces are presented in Table 7. The diagrams of these forces along the cross-sections of the structure are shown in Fig. 5. The convention adopted for drawing the diagrams of shear forces is such that positive values are drawn on the side of the upper fibers of the bar, being represented in turquoise, and negatives on the other side, being represented in magenta. In the diagrams of normal forces, the positive values of the normal force (traction) are represented in turquoise and negative values of the normal force (compression) are in magenta.

Regarding the shearing forces, for CI its maximum value is equal to 3.553 kN, while for CII it is 2.876 kN, and for CIII it is 3.949 kN (Table 7).

Regarding the normal forces, for CI and CII their maximum value for the cables is 2.093 kN and for CIII it is 1.674 kN (Table 7).

Considering the columns (elements A and E), the maximum value of the normal force for CI is -36.975 kN,

**Table 7 Values of shear and normal forces.**

| Element | Shear force (kN) | | | Normal force (kN) | | |
|---|---|---|---|---|---|---|
| | CI | CII | CIII | CI | CII | CIII |
| A | 0.386 | 0.313 | -3.278 | -36.975 | -30.304 | 27.443 |
| B | 0.000 | 0.000 | 0.000 | 2.093 | 2.093 | 1.674 |
| C | -0.217 | -0.188 | -0.093 | -18.098 | -14.676 | 8.1460 |
| D | -0.079 | -0.073 | -0.203 | -19.320 | -15.663 | 22.192 |
| E | -0.084 | -0.069 | 3.919 | -4.358 | -3.804 | 1.845 |
| F | 0.491 | 0.412 | -0.566 | -17.658 | -14.263 | 7.646 |
| G | 0.217 | 0.190 | -0.792 | 0.844 | 0.724 | -0.391 |
| H | 0.074 | -0.072 | -0.733 | -1.771 | -1.344 | 3.201 |
| I | -0.096 | -0.091 | 0.113 | -11.652 | -9.479 | 12.515 |
| J | -3.186 | -2.579 | 3.462 | 2.584 | 1.993 | -6.118 |
| K | 2.880 | 2.334 | -3.357 | 5.487 | 4.273 | -6.223 |
| L | -0.205 | -0.200 | 0.179 | -7.615 | -6.059 | 11.349 |
| M | 0.000 | 0.000 | 0.000 | 1.872 | 1.872 | 1.497 |
| N | 2.865 | 2.313 | -3.227 | -4.441 | -3.773 | 4.606 |
| O | 0.330 | 0.317 | -0.276 | -13.751 | -11.545 | 10.898 |
| P | -3.553 | -2.876 | 3.949 | 8.644 | 7.389 | -2.570 |
| Q | 0.214 | 0.193 | -0.201 | -10.822 | -8.790 | 11.797 |
| R | 3.456 | 2.788 | -3.924 | 20.647 | 17.139 | -15.682 |

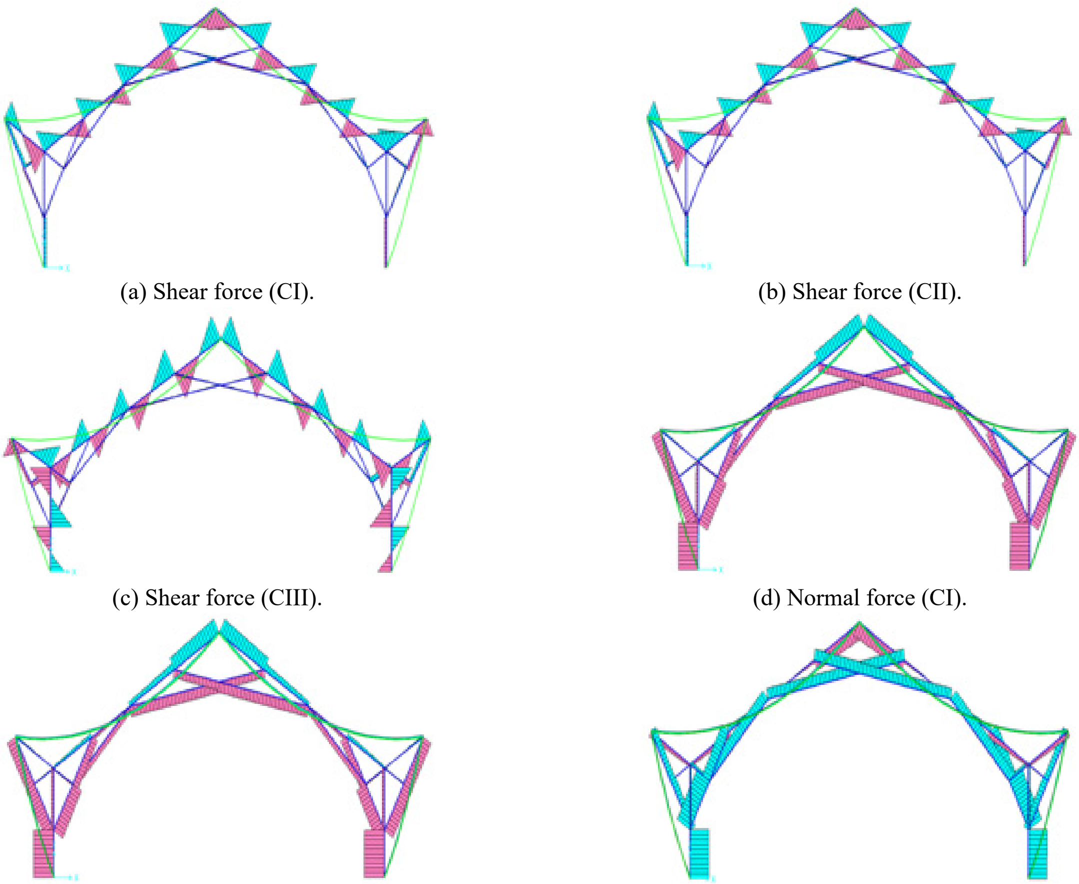

(a) Shear force (CI).
(b) Shear force (CII).
(c) Shear force (CIII).
(d) Normal force (CI).
(e) Normal force (CII).
(f) Normal force (CIII).

**Fig. 5 Diagram of shear and normal forces.**

and for CII it is -30.304 kN, both compressive forces. For CIII it is 27.443 kN, a traction force (Table 7).

Considering the beams (elements C, D, F, G, H, I, J, K, L, N, O, P, Q, and R), the maximum value of the tractive force for CI is 20.647 kN, for CII it is 17.139 kN, and for CIII it is 22.192 kN. The maximum value of the compressive force for CI is 36.975 kN, for CII it is 30.304 kN, and for CIII it is 15.682 kN (Table 7).

Analyzing the capacity of the structure in relation to shear, as well as in relation to the normal traction and compression stress of the columns and beams, with rectangular sections of 100 mm × 60 mm /3 mm and 80 mm × 60 mm / 3 mm, it is observed that all elements comply the established safety mode.

### *4.2 Requesting Efforts (Bending Moment and Normal Stress)*

The values of bending moments and maximum normal stresses are presented in Table 8. The diagrams of these efforts along the cross-sections of the structure are shown in Fig. 6. The convention adopted for drawing the bending moment diagrams is such that positive values of bending moments are drawn on the side of the lower fibers of the bar, being represented in turquoise color, and negative moments on the other side, being represented in magenta color. In normal stress diagrams, the turquoise color represents tractive stress and the magenta color represents compressive stress.

Regarding the maximum values of the bending moments, it can be seen that, in the case of columns, for the CI the maximum value is 0.485 kN·m, for CII it is 0.393 kN·m, and for CIII it is 2.151 kN·m.

In the case of 100 × 60 beams, for the CI the maximum value of the bending moment is -2.507 kN·m, for CII it is 2.024 kN·m, and for CIII it is 2.868 kN·m. In the case of 80 × 60 beams, for the CI the maximum value of the bending moment is -0.508 kN·m, for CII it is 0.465 kN·m, and for CIII it is 0.466 kN·m.

Regarding the values of the maximum normal stresses, for the CI the maximum value of the normal stress is 117.499 MPa, for CII it is 94.745 MPa, and for CIII it is 101.313 MPa.

**Table 8 Values of bending moments and normal stresses.**

| Element | Bending moments (kN·m) | | | Normal stresses (MPa) | | |
|---|---|---|---|---|---|---|
| | CI | CII | CIII | CI | CII | CIII |
| A | 0.485 | 0.393 | -1.788 | -39.779 | -32.598 | 100.524 |
| B | 0.000 | 0.000 | 0.000 | 0.000 | 0.000 | 0.000 |
| C | -0.242 | -0.201 | 0.106 | -18.847 | -15.401 | 12.821 |
| D | -0.128 | -0.108 | -0.259 | -18.388 | -14.878 | 34.079 |
| E | 0.164 | 0.135 | -2.151 | -4.355 | -3.791 | 86.930 |
| F | 0.806 | 0.650 | -1.038 | -17.916 | -14.738 | 49.389 |
| G | -0.182 | -0.151 | -0.770 | 8.028 | 6.661 | 30.131 |
| H | -0.110 | -0.096 | 0.784 | 2.524 | 2.338 | 34.518 |
| I | -0.072 | -0.061 | 0.101 | -12.429 | -9.848 | 17.526 |
| J | -1.987 | -1.608 | 1.907 | 77.946 | 62.965 | 72.926 |
| K | -1.690 | -1.371 | 2.185 | 69.337 | 56.055 | 83.827 |
| L | -0.205 | -0.194 | -0.230 | -7.685 | -6.202 | 21.386 |
| M | 0.000 | 0.000 | 0.000 | 0.000 | 0.000 | 0.000 |
| N | -1.600 | -1.291 | 1.767 | 58.580 | 47.060 | 74.976 |
| O | -0.508 | -0.465 | -0.466 | -16.529 | -13.921 | 38.752 |
| P | -2.499 | -2.024 | 2.706 | 108.344 | 88.157 | 104.402 |
| Q | -0.268 | -0.221 | -0.162 | -13.305 | -10.857 | 23.479 |
| R | -2.507 | -2.008 | 2.868 | 117.499 | 94.745 | 101.313 |

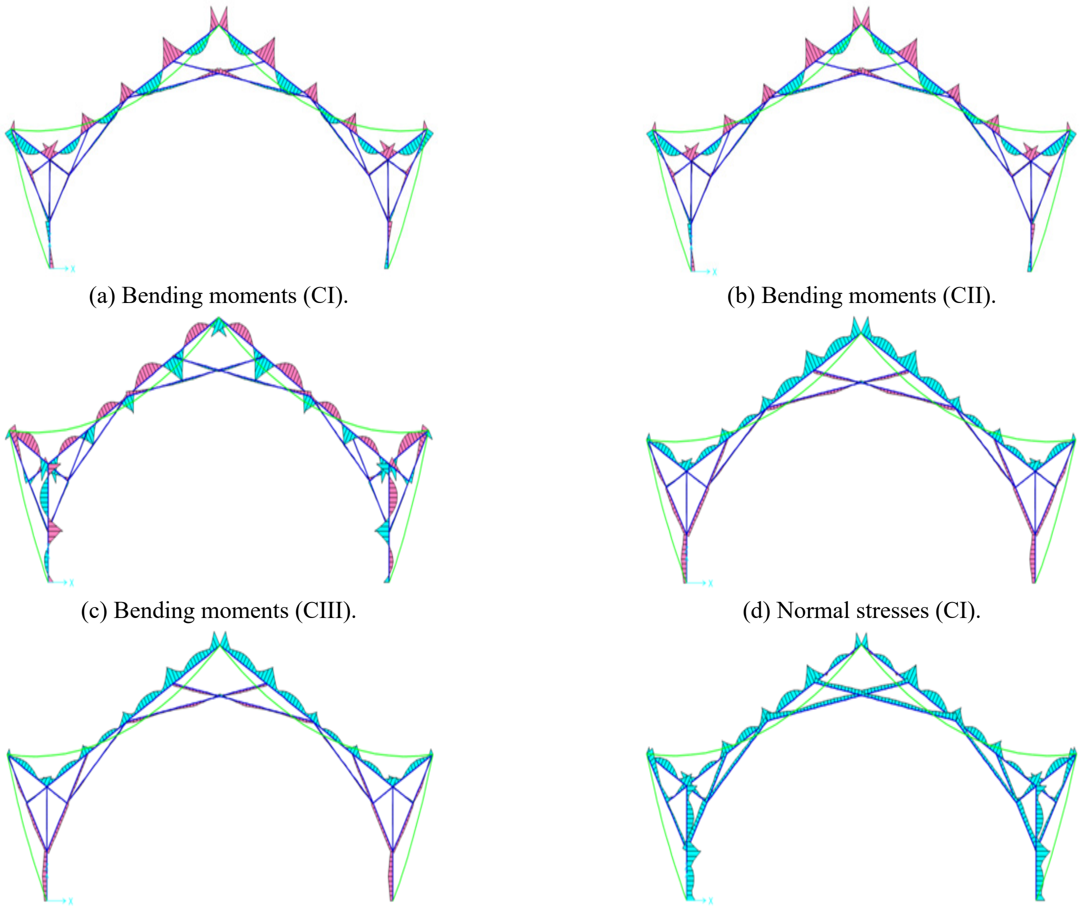

(a) Bending moments (CI). (b) Bending moments (CII).

(c) Bending moments (CIII). (d) Normal stresses (CI).

(e) Normal stresses (CII). (f) Normal stresses (CIII).

**Fig. 6 Diagram of bending moments and normal stresses.**

It is observed that with the initial tension applied to the cables at the discriminated values, the normal tractive stresses are zero.

Safety is checked regarding the bending moment in columns and beams with rectangular sections of 100 mm × 60 mm / 3 mm and 80 mm × 60 mm / 3 mm and it is observed that all these elements comply with the established safety mode. The safety of the composite bending with compression and composite bending with shear stress in the beams is also verified.

It is still verified that the normal stresses do not exceed the value of the yield strength of stainless steel, which is 400 MPa.

*4.3 Displacements*

The values of the maximum expected displacements, considering the SLS (service limit state), are presented in Table 9. The diagrams of the displacements of the structure bars are shown in Fig. 7. The scale next to these figures indicates the amplitude of the displacements (in mm), which is also shown in color, ranging from blue (lower values) to purple (higher values), showing the most critical regions of the structure. The cables are represented in black to differentiate from the displacements obtained in the other elements.

Regarding the bars, the highest value obtained for the displacement in a column (horizontal) is 0.95 mm in bar E, combination FC2, while the highest value obtained for the displacement in a beam (vertical) is 3.33 mm in bar O, combination FC1 Thus, in both cases, the displacement values are considerably lower than those allowed, which are 38.87 mm for horizontal displacement and 125 mm for vertical displacement.

**Table 9 Maximum displacement values (mm).**

| Element | APC | FC1 | FC2 | Element | APC | FC1 | FC2 |
|---|---|---|---|---|---|---|---|
| A | 0.47 | 0.59 | 0.26 | J | 0.83 | 1.05 | -0.14 |
| B | 54.13 | 53.17 | 55.17 | K | 0.88 | 1.12 | 0.17 |
| C | 0.47 | 0.59 | 0.27 | L | 1.34 | 1.59 | 0.73 |
| D | -0.34 | -0.44 | -0.21 | M | 121.97 | 121.87 | 122.55 |
| E | 0.47 | 0.59 | 0.95 | N | 1.35 | 1.80 | 0.11 |
| F | 0.34 | 0.42 | 0.08 | O | 3.22 | 3.33 | 2.96 |
| G | 0.09 | 0.11 | -0.05 | P | 1.84 | 2.35 | 0.28 |
| H | 0.42 | 0.52 | 0.15 | Q | 0.22 | -0.44 | 0.79 |
| I | 0.48 | 0.63 | 0.13 | R | 0.95 | 1.14 | 0.29 |

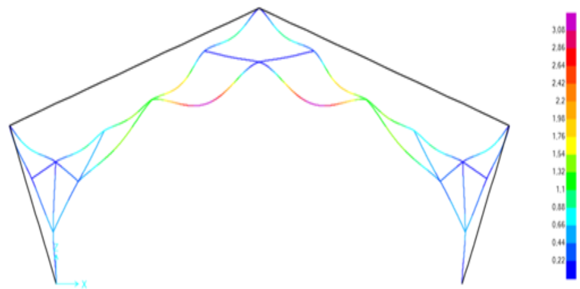

(a) Displacement (APC).

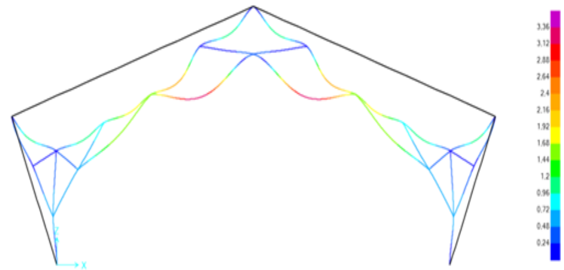

(b) Displacement (FC1).

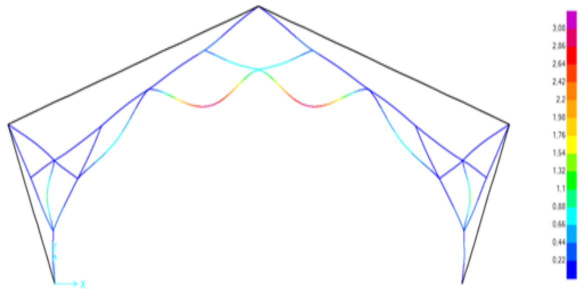

(c) Displacement (FC2).

**Fig. 7 Displacement diagrams.**

The displacements of the cables, elements B and M, in the form of a catenary, have their highest values equal to 55.17 mm in cable B and 122.55 mm in cable M, both for the FC2 combination, and are consistent with the values of the initial stresses associated to them and consistent with the general configuration of the structure.

*4.4 Cost Analysis*

To verify the economic feasibility of using stainless steel as a replacement for ASTM A36 steel, a cost analysis of the original structure and the proposed structure is performed, based on the average between the highest and lowest quoted commercial price. The price survey is carried out in the last week of June 2020 at distributors and stores located in the southeast region of Brazil, preserving their identity. This region was chosen because it is where the reference gymnasiums are located. The variation of the dollar in the week of the price survey is high due to the COVID-19 pandemic, but it impacted both types of steel in question, not benefiting one or the other.

The average market price was US \$0.83/kg of ASTM A36 steel and US \$3.24/kg of AISI 304 stainless steel. The cost analysis shows that AISI 304 stainless steel is approximately four times more expensive than ASTM A36 steel, which proves the need to propose a lighter structure so that its use is

**Table 10 Commercial price survey.**

| Structure type | Value (US $) |
|---|---|
| Original ASTM A36 steel structure | 2,071.60 |
| Original AISI 304 stainless steel structure | 8,116.13 |
| Proposed AISI 304 stainless steel structure | 3,425.98 |

Source: Oliveira [6].

more viable. The steel arched structure in ASTM A36 steel weighs 2,502 kg, as described in the structural design of the building, according to Santos [5], and the portico of the proposed AISI 304 stainless steel structure weighs 1,056.76 kg, according to the structural study presented (Table 2), that is, there is a significant reduction of 57.76% in the weight of the structure. Table 10 shows the average prices of the original structure in ASTM A36 steel, the original structure in AISI 304 stainless steel, and the proposed structure in AISI 304 stainless steel.

It is observed that the value of the original structure in ASTM A36 steel is 25% of the value of the original structure if it were in AISI 304 stainless steel. However, the proposed stainless steel structure would cost 42% of the original structure in AISI 304 stainless steel, thus increasing the viability of stainless steel if used in the proposed structure.

## 5. Conclusion

The guidelines that defined the essence of the proposed project took into account the three main pillars of good architecture: functionality, aesthetics, and financial viability. The project leads to spaces favorable to the practice of sports, the main activity carried out in this type of building, but it also presents a modern and imposing volume try, referring to the characteristics of the material used. Finally, it presents itself as economically viable from the use of profiles that make the structure approximately 58% lighter when compared to the structure of the gymnasiums taken as a reference, thus reducing its cost in relation to common steel.

The design of a building taking into account the use of materials already established in other areas, but still innovative in civil construction, which is the case of stainless steel in closure systems and structures, tend to be increasingly common, and proposals that unite architecture and engineering in the sense of accomplishing these goals, such as the one presented in this work, tend to contribute in this aspect. It is also important that architecture presents itself as a significant element, playing the role of an engineering partner so that both grow and develop together.

## Acknowledgments

The authors thank the UFOP (Federal University of Ouro Preto) and the CAPES (Coordination for the Improvement of Higher Education Personnel), Brazil.

## References

[1] Baddoo, N. R., and Burgan, B. 2001. *Structural Design of Stainless Steel.* London: Steel Construction Institute. ISBN: 1 85942 116 4.

[2] Gedge, G. 2008. "Structural Uses of Stainless Steel—Buildings and Civil Engineering." *Journal of Constructional Steel Research* 64 (11): 1194-8. doi: 10.1016/j.jcsr.2008.05.006.

[3] Corradi, M., Schino, A., Borri, A., and Rufini, R. 2018. "A review of the use of stainless steel for masonry repair and reinforcement." *Construction and Building Materials* 181: 335- 346. doi: 10.1016/j.conbuildmat.2018.06.034.

[4] Gardner, L. 2005. "The Use of Stainless Steel in Structures." *Progress in Structural Engineering and Materials* 7 (2): 45-55. doi: 10.1002/pse.190.

[5] Santos, R. W. 2003. Cobertura em Estruturas Metálicas: projeto & cálculo. *RWS Engenharia Ltda*. Timóteo, MG, Brasil. (in Portuguese)

[6] Oliveira, G. D. 2020. "Alternativa arquitetônica projetual de estrutura de cobertura em aço inoxidável para edificações cobertas por telhas de aço inoxidável." Ph.D. thesis, Universidade Federal de Ouro Preto. (in Portuguese)

[7] Solidworks. 2019. *Dessault Systèmes*. Biblioteca técnica. Accessed on March 3, 2019. https://www.ssab.com.br/support/calculators-and-tools/material-library-for-solidworks-by-dassault-systemes. (in Portuguese)

[8] ABNT—Associação Brasileira de Normas Técnicas 2019. *NBR ISO 2408: Cabos de Aço e Acessórios*. Rio de Janeiro: ABNT. (in Portuguese)

[9] Nunes, E. F. 2008. "Tensoestruturas—Elementos e cabos

metálicos associados a membranas." M.Sc. thesis, Universidade Federal de Ouro Preto. http://www.repositorio.ufop.br/jspui/handle/123456789/2261. (in Portuguese)

[10] European Standard. 2005. *EN 1993-1-1, Eurocode 3: Design of Steel Structures: General Rules and Rules for Buildings*.

[11] European Standard. 2006. *EN 1993-1-3, Eurocode 3: Design of Steel Structures: General Rules—Supplementary Rules for Cold-Formed Members and Sheeting*.

[12] European Standard. 2006. *EN 1993-1-4, Eurocode 3: Design of Steel Structures: General Rules—Supplementary Rules for Stainless Steels*.

[13] European Standard. 2006. *EN 1993-1-5, Eurocode 3: Design of Steel Structures: Plated Structural Elements*.

[14] European Standard. 2005. *EN 1993-1-8, Eurocode 3: Design of Steel Structures: Design of Joints*.

[15] ABNT—Associação Brasileira de Normas Técnicas 2008. *NBR 8800: Projeto de estruturas de aço e de estruturas mistas de aço e concreto de edifícios.* Rio de Janeiro: ABNT. (in Portuguese)